Co–Au core-shell nanocrystals formed by sequential ion implantation into SiO_2

P. Kluth,[a] B. Hoy, B. Johannessen, and S. G. Dunn
Department of Electronic Materials Engineering, Australian National University, Canberra ACT 0200, Australia

G. J. Foran
Australian Nuclear Science and Technology Organization, Menai, NSW 2234 Australia

M. C. Ridgway
Department of Electronic Materials Engineering, Australian National University, Canberra ACT 0200, Australia

(Received 24 May 2006; accepted 23 August 2006; published online 12 October 2006)

Co–Au core-shell nanocrystals (NCs) were formed by sequential ion implantation of Au and Co into thin SiO_2. The NCs were investigated by means of transmission electron microscopy and extended x-ray absorption fine structure spectroscopy. The latter reveals a bond length expansion in the Co core compared to monatomic Co NCs. Concomitantly, a significant contraction of the bond length and a significant reduction of the effective Au–Au coordination number were observed in the Au shells. Increased Debye-Waller factors indicate significant strain in the NCs. These experimental results verify recent theoretical predictions. © *2006 American Institute of Physics*.
[DOI: 10.1063/1.2360891]

Nanocrystals (NCs) have received increasing attention due to their unique properties and their wide range of prospective applications. Metallic NCs embedded in a dielectric matrix are particularly interesting because of their optical properties with a high potential for application in optical filters, memories, or switching devices.[1]

Ion implantation is a very versatile technique and has been used to synthesize NCs for over three decades. Sequential implantation of two metals has been studied in recent years to form mixed NC systems. Using a combination of two different metals provides a means of controlled tuning of the optical properties of the NC composite material. Three types of NC arrangements can principally be obtained by sequential implantation: separated monoelemental NCs, alloy-based NCs, or core-shell structures, where one material forms a solid core and the other a surrounding shell. Core-shell structures are particularly interesting due to the change in dielectric constant at the core-shell boundary.[1] The majority of investigated material systems show alloyed NC formation (for example, Au–Ag, Au–Cu, Cu–Ni, and Ni–Co).[2] Core-shell NCs have been reported for the Ag–Cu system,[3] the Ag–S system (as Ag cores with Ag_2S shells[4]), the Fe–Al system,[5] and the Pd–Cu system (as Pd rich cores with CuO shells).[6]

In the present letter, we demonstrate the formation of Co–Au core-shell NCs in thin SiO_2 fabricated by sequential ion implantation of Au and Co. The NCs were investigated by means of cross-sectional transmission electron microscopy (TEM) and extended x-ray absorption fine structure (EXAFS) spectroscopy. EXAFS provides a powerful tool for structural analysis of particles of nanometer dimensions,[7] giving unique information about the local atomic environment of the absorbing atom. The technique is particularly sensitive to interatomic distances and local disorder. We have studied the local atomic structure of the Co–Au core-shell NCs and compared the results to monatomic Au and Co NCs fabricated under identical conditions. Our measurements show striking similarities with recent simulations on Co–Ag nanocrystals which represent a similar materials system.

For the NC synthesis, we first implanted 1.2 MeV ^{197}Au ions with a total fluence of 5×10^{16} ions/cm^2 into $\sim$0.6 μm thick SiO_2. The SiO_2 was thermally grown on Si (100) substrates. Implantation was carried out at room temperature. The samples were then annealed in O_2 at 1000 °C for 1 h in a conventional quartz tube furnace (O_2 enhances the growth of Au NCs).[8] Subsequently, samples were implanted with 350 keV ^{59}Co ions with a fluence of 8×10^{16} ions/cm^2. The fluence was chosen to approximately match the peak concentration of Au. Co implantation was performed at 400 °C to promote atomic diffusion and structural rearrangement of the metal atoms. Simultaneously, Co was implanted into unimplanted SiO_2. No subsequent annealings were performed.

To prepare the samples for the EXAFS measurements, the thin SiO_2 layer containing the NCs was isolated by removing the Si substrate via mechanical polishing and selective wet chemical etching. Multiple layers of the thin implanted SiO_2 were then mounted on a sample holder. Using this sample preparation method, we enhance the relative metal concentration and eliminate scattering from the substrate.

EXAFS measurements were performed in fluorescence mode at the Au L_3 edge (11.919 keV) and the Co K edge (7.709 keV) at the Photon Factory, Japan (beamline 20-B). Data were collected using a ten-element Ge solid state detector. The fluorescence signal comprised between 10% and 50% of the incoming count rate, with the latter maintained well within the linear region of the detector. Measurements were carried out at a temperature of 10 K to reduce thermal vibrations. Thin Au (100 nm) and Co (20 nm) films were measured as references.

The spectra were analyzed using the FEFFIT program package.[9] EXAFS spectra recorded at the Au L_3 and the Co K edge were Fourier transformed (FT) over a k range of 4.7–15 and 3.0–13.5 $Å^{-1}$, respectively. Structural parameters

[a]Electronic mail: patrick.kluth@anu.edu.au

 © 2006 American Institute of Physics
Downloaded 13 Oct 2006 to 150.203.178.77. Redistribution subject to AIP license or copyright, see http://apl.aip.org/apl/copyright.jsp

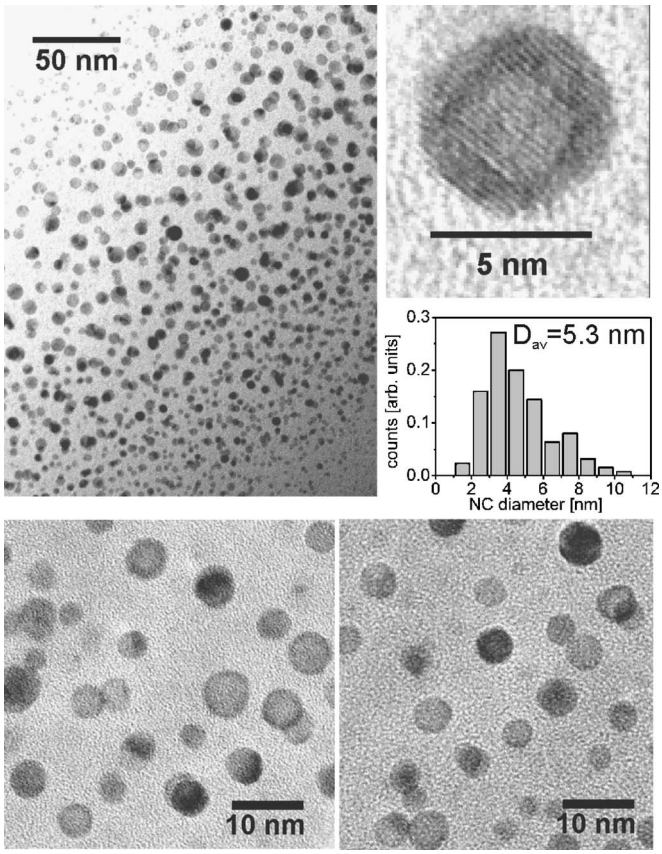

FIG. 1. Cross-sectional TEM images and size distribution of Co–Au NCs. The lower panels show the existence of Co–Au core-shell NCs as well as monoelemental NCs. The high-resolution image of a Co–Au core-shell NC reveals a significant bending of the lattice fringes consistent with high strain.

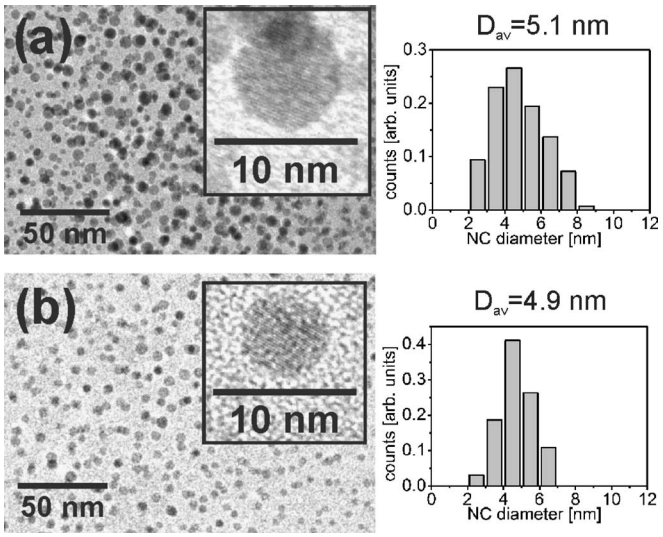

FIG. 2. Cross-sectional TEM images and size distributions of (a) Au NCs and (b) Co NCs.

were extracted from the first coordination shell which was isolated by inverse transforming over a non-phase-corrected radial distance range of 2.1–3.2 Å for the Au L_3 edge and 1.65–2.7 Å for the Co K edge. The spectra were then fitted to the EXAFS equation.[10] The amplitude reduction factors (S_0^2) and threshold energies (E_0) were determined from the thin metal films and kept constant for fitting the NC spectra. The photoelectron scattering-path amplitudes and phases were calculated *ab initio* using FEFF8.[11]

Figure 1 shows cross-sectional TEM images of the sequentially implanted Au–Co sample. The NC size distribution extracted from TEM shows a volume weighted average particle diameter of 5.3 nm. The two images in the lower panel clearly illustrate the formation of Co–Au core-shell NCs identified by the darker Au shells surrounding the lighter Co cores. Simultaneously, we also observe the presence of monoelemental Co and Au NCs. In the high-resolution image we can see a significant bending of the lattice fringes in the Au shell, which is consistent with strain in the core-shell NCs. Figure 2 shows TEM images of monoelemental (a) Au and (b) Co NCs formed by single implants. Both show spherical, largely single-crystalline NCs with (volume-weighted) average diameters of 5.1 and 4.9 nm, respectively, slightly smaller than the 5.3 nm for the core-shell sample. Electron diffraction (not shown) confirms the face-centered-cubic structure dominates for Au, Co, and core-shell NCs.

Figure 3 shows the Fourier transformed EXAFS spectra (a) of the Au film, Au NCs, and the core-shell NCs at the Au L_3 edge and (b) of the Co film, the Co NCs, and the core-shell NCs at the Co K edge. The solid lines show the corresponding first shell fits. The refined fitting parameters are given in Table I. The insets in Fig. 3 show Debye-Waller factors and bond lengths as given in Table I. The NC spectra at the Au L_3 edge exhibit reduced amplitudes compared to the Au film spectrum. This reflects the decrease in average coordination number (CN) and increase in Debye-Waller factor, both resulting from the increased surface to bulk ratio (SBR) inherent with NCs. The atoms at the NC surface are undercoordinated and as a consequence relaxed or reconstructed. The former yields the reduction in average CN and the latter leads to an increase in Debye-Waller factor. For the

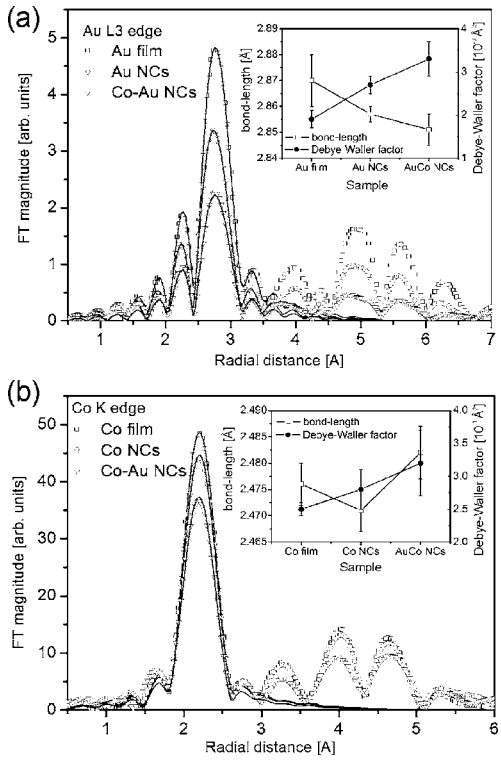

FIG. 3. Non-phase corrected Fourier transformed EXAFS spectra of (a) Au film, Au NCs, and Co–Au NCs at the Au L_3 edge (k^2 weighted) and (b) Co film, Co NCs, and Co–Au NCs at the Co K edge (k^3 weighted). The solid lines show the corresponding first-shell fits. The insets show bond lengths and Debye-Waller factors as given in Table I.

Downloaded 13 Oct 2006 to 150.203.178.77. Redistribution subject to AIP license or copyright, see http://apl.aip.org/apl/copyright.jsp

TABLE I. Refined fitting parameters from EXAFS analysis of the first coordination shell of metal film and NC samples. N, R, and σ^2 are the coordination number, bond length, and Debye-Waller factor, respectively.

Sample	Absorption edge	N	R (Å)	σ^2 (10^{-3} Å^2)
Au film	Au L_3	12 (fixed)	2.870±0.01	1.9±0.2
Co film	Co K	12 (fixed)	2.476±0.004	2.5±0.1
Au NCs	Au L_3	10.4±0.6	2.857±0.003	2.7±0.2
Co NCs	Co K	11.5±0.7	2.471±0.004	2.8±0.3
Co–Au NCs	Au L_3	8.0±0.9	2.851±0.006	3.3±0.4
	Co K	10.6±0.8	2.482±0.005	3.2±0.5

monoelemental Au NCs, the CN of 10.4±0.6 is in reasonable agreement with a value of 11.0 calculated for a 5.1 nm NC using an approximation for spherical 12-fold coordinated particles given by $CN_{NC}=12(1-(3/2D)R_{nn})$,[12] where R_{nn} is the nearest neighbor distance and D the NC diameter. The significantly reduced Au–Au CN of 8.0 in the core-shell NCs is consistent with an expected reduction due to the greatly increased SBR of the Au shells which effectively comprise of a hollow sphere. TEM images indicate that the Au shells are approximately 1–2 nm thick and are thus undercoordinated on both the interior and exterior of the shell. The amplitudes in the FT spectra for samples measured at the Co K edge vary to a much lesser extend as compared to those of Au. A slightly reduced CN of the core-shell NCs (10.6) compared to the monoelemental Co NCs (11.5) is consistent with a reduced average diameter of the Co cores relative to the average monoelemental Co NC diameter as indicated by TEM.

The Co–Co bond length in the core-shell NCs is expanded by 0.5% relative to that of the monoelemental Co NCs. This also exceeds the bond length of the Co film. Generally, monoelemental metal NCs exhibit a bond-length contraction compared to the bulk due to surface tension effects as shown here for both Co and Au and previously for ion implanted Au and Cu NCs.[13] A further difference is manifested in the significantly increased Debye-Waller factor in the core-shell NCs, representing a broadening of the bond-length distribution. Both the increased Debye-Waller factor and bond-length expansion are consistent with an increased strain present in the NCs which was also apparent from the high-resolution TEM image as mentioned earlier. The Au–Au bond-length contraction and Co–Co bond-length expansion in the core-shell NCs, relative to the monoelemental NCs, are consistent with the significant lattice mismatch between the two metals. The spectra of the core-shell NCs show no significant indication of Au–Co bonding (at both Au L_3 and Co K edges), indicating the absence of alloyed phases in the sample. Bonding of Au and Co is only expected at the core-shell interface. Such bonds comprise a small fraction of total bonds and are expected to be disordered due to the large mismatch and the associated strain. Thus no contribution of such bonding is apparent in the FT EXAFS spectra. We note that the coexistence of core-shell and monoelemental NCs in the core-shell sample makes a quantitative interpretation of the structural parameters obtained by EXAFS difficult as EXAFS averages over all NCs; however, it also means that the observed striking differences compared to the monoelemental samples are somewhat underestimated.

The formation of the core-shell structures can be explained by a minimization of the surface-free energy which promotes the segregation of Au at the Co surface. The gain has to outweigh the increase in energy due to the increased strain which will ultimately impose limits for the composition and size of the core-shell NCs. Recently, simulations on the thermodynamic equilibrium state structure of Co–Ag NCs—a very similar system to that studied in this report (both systems show the tendency toward phase separation in the bulk phase)—were reported.[14] The simulations predict the formation of Co–Ag core-shell structures, the expansion of the Co–Co bonds induced by the Ag shells, and strain in the NCs. These observations are in very good agreement with our experimental results. Although fabrication conditions, in particular using ion implantation, are often far from equilibrium, an elevated temperature during the second implant can enable sufficient mobility of the atoms for the formation of these equilibrium structures.

In conclusion we have observed the formation of Co–Au core-shell NCs following sequential ion implantation of Au and Co. The Au–Au bonds of the shell contract while the Co–Co bonds of the core expand compared to monoelemental Au and Co NCs. Furthermore, a significantly increased strain is apparent in the NCs. The observations are in very good agreement with simulations of the equilibrium structure of Co–Ag core-shell NCs.

P.K. and M.C.R. thank the Australian Research Council for support. P.K., B.H., B.J., and M.C.R. were supported by the Australian Synchrotron Research Program, funded by the Commonwealth of Australia via the Major National Research Facilities Program.

[1] A. Meldrum, L. A. Boatner, and C. W. White, Nucl. Instrum. Methods Phys. Res. B **178**, 7 (2001).
[2] G. Mattei, Nucl. Instrum. Methods Phys. Res. B **191**, 323 (2002).
[3] T. S. Anderson, R. H. Magruder Iii, J. E. Wittig, D. L. Kinser, and R. A. Zuhr, Nucl. Instrum. Methods Phys. Res. B **171**, 401 (2000).
[4] E. Cattaruzza, G. Battaglin, R. Polloni, T. Cesca, F. Gonella, G. Mattei, C. Maurizio, P. Mazzoldi, F. D'Acapito, F. Zontone, and R. Bertoncello, Nucl. Instrum. Methods Phys. Res. B **148**, 1007 (1999).
[5] C. de Julian Fernandez, M. A. Tagliente, G. Mattei, C. Sada, V. Bello, C. Maurizio, G. Battaglin, C. Sangregorio, D. Gatteschi, L. Tapfer, and P. Mazzoldi, Nucl. Instrum. Methods Phys. Res. B **216**, 245 (2004).
[6] G. Mattei, C. Maurizio, P. Mazzoldi, F. D'Acapito, G. Battaglin, E. Cattaruzza, C. d. Julian Fernandez, and C. Sada, Phys. Rev. B **71**, 195418 (2005).
[7] A. I. Frenkel, C. W. Hills, and R. G. Nuzzo, J. Phys. Chem. B **105**, 12689 (2001).
[8] A. Miotello, G. De Marchi, G. Mattei, P. Mazzoldi, and C. Sada, Phys. Rev. B **63**, 075409 (2001).
[9] M. Newville, B. Ravel, D. Haskel, J. J. Rehr, E. A. Stern, and Y. Yacoby, Physica B **208/209**, 154 (1995).
[10] E. A. Stern, Phys. Rev. B **10**, 3027 (1974).
[11] A. L. Ankudinov, B. Ravel, J. J. Rehr, and S. D. Conradson, Phys. Rev. B **58**, 7565 (1998).
[12] S. de Panfilis, F. d'Acapito, V. Haas, H. Konrad, J. Weissmuller, and F. Boscherini, Phys. Lett. A **207**, 397 (1995).
[13] P. Kluth, B. Johannessen, V. Giraud, A. Cheung, C. J. Glover, G. de M. Azevedo, G. J. Foran, and M. C. Ridgway, Appl. Phys. Lett. **85**, 3561 (2004); B. Johannessen, P. Kluth, C. J. Glover, G. de M. Azevedo, D. J. Llewellyn, G. J. Foran, and M. C. Ridgway, J. Appl. Phys. **98**, 024307 (2005).
[14] T. Van Hoof and M. Hou, Phys. Rev. B **72**, 115434 (2005).

Downloaded 13 Oct 2006 to 150.203.178.77. Redistribution subject to AIP license or copyright, see http://apl.aip.org/apl/copyright.jsp